Article

Cell Metabolism

Phosphoproteomics Identifies CK2 as a Negative Regulator of Beige Adipocyte Thermogenesis and Energy Expenditure

Graphical Abstract

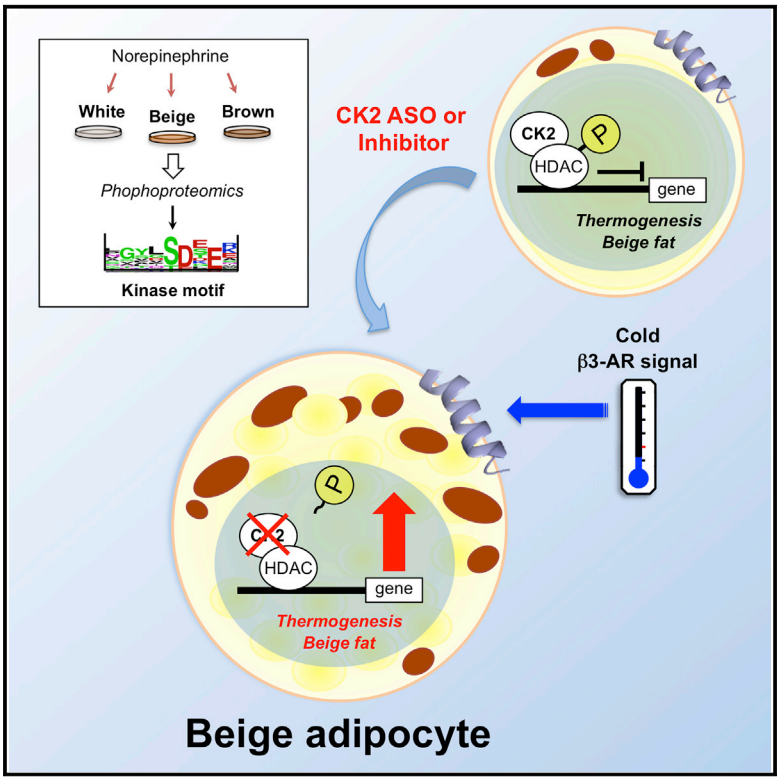

Highlights

- CK2 is preferentially activated in white fat by norepinephrine and under obesity
- CK2 inhibition in white fat activates thermogenesis in response to cAMP stimuli
- CK2 inhibition increases UCP1-dependent energy expenditure in vivo
- CK2 inhibition ameliorates diet-induced obesity and insulin resistance

Authors

Kosaku Shinoda, Kana Ohyama, Yutaka Hasegawa, ..., Mark Graham, Yasushi Ishihama, Shingo Kajimura

Correspondence

skajimura@diabetes.ucsf.edu

In Brief

Kajimura et al. map global and temporal phosphorylation profiles in brown, beige, and white adipocytes following adrenergic stimulation and reveal that the Caseine K2 (CK2) pathway is preferentially activated in WAT. Genetic or pharmacological CK2 inhibition in WAT promotes beige adipogenesis and thermogenesis in vivo and ameliorates diet-induced obesity.

Shinoda et al., 2015, Cell Metabolism 22, 997–1008
December 1, 2015
http://dx.doi.org/10.1016/j.cmet.2015.09.029

Cell Metabolism
Article

Phosphoproteomics Identifies CK2 as a Negative Regulator of Beige Adipocyte Thermogenesis and Energy Expenditure

Kosaku Shinoda,[1] Kana Ohyama,[1] Yutaka Hasegawa,[1] Hsin-Yi Chang,[2] Mayu Ogura,[2] Ayaka Sato,[2] Haemin Hong,[1] Takashi Hosono,[1] Louis Z. Sharp,[1] David W. Scheel,[1] Mark Graham,[3] Yasushi Ishihama,[2] and Shingo Kajimura[1,*]
[1]UCSF Diabetes Center and Department of Cell and Tissue Biology, University of California, San Francisco, 35 Medical Center Way, San Francisco, CA 94143-0669, USA
[2]Department of Molecular and Cellular Bioanalysis, Graduate School of Pharmaceutical Sciences, Kyoto University, Kyoto 606-8501, Japan
[3]Cardiovascular Group, Department of Antisense Drug Discovery, Isis Pharmaceuticals, Inc., Carlsbad, CA 92008, USA
*Correspondence: skajimura@diabetes.ucsf.edu
http://dx.doi.org/10.1016/j.cmet.2015.09.029

SUMMARY

Catecholamines promote lipolysis both in brown and white adipocytes, whereas the same stimuli preferentially activate thermogenesis in brown adipocytes. Molecular mechanisms for the adipose-selective activation of thermogenesis remain poorly understood. Here, we employed quantitative phosphoproteomics to map global and temporal phosphorylation profiles in brown, beige, and white adipocytes under β3-adrenenoceptor activation and identified kinases responsible for the adipose-selective phosphorylation profiles. We found that casein kinase2 (CK2) activity is preferentially higher in white adipocytes than brown/beige adipocytes. Genetic or pharmacological blockade of CK2 in white adipocytes activates the thermogenic program in response to cAMP stimuli. Such activation is largely through reduced CK2-mediated phosphorylation of class I HDACs. Notably, inhibition of CK2 promotes beige adipocyte biogenesis and leads to an increase in whole-body energy expenditure and ameliorates diet-induced obesity and insulin resistance. These results indicate that CK2 is a plausible target to rewire the β3-adrenenoceptor signaling cascade that promotes thermogenesis in adipocytes.

INTRODUCTION

A chronic imbalance between energy intake and energy expenditure leads to the development of obesity and metabolic diseases, including type 2 diabetes. While decreasing food intake and increasing physical activity constitute logical ways to tip energy balance toward weight loss in the short term, effective and alternative approaches are warranted for long-term maintenance of proper body weight. Since the prevalence of brown adipose tissue (BAT) and its contribution to energy homeostasis have been widely appreciated in adult humans, it is considered that increasing BAT-mediated thermogenesis via uncoupling protein 1 (UCP1) serves as an alternative approach to modulate energy balance (reviewed in Sidossis and Kajimura, 2015).

Recent studies suggest that rodents and humans possess at least two populations of UCP1-positive thermogenic adipocytes: classical brown adipocytes and beige adipocytes (or brite cells). Beige adipocytes reside sporadically within white adipose tissue (WAT) where they emerge in response to certain external stimuli, such as chronic cold exposure, exercise, and long-term treatment with PPARγ agonists. This phenomenon is often referred to as the "browning" of WAT (reviewed in Harms and Seale, 2013; Kajimura and Saito, 2014). Recent studies using ^{18}F-fluoro-2-deoxy-d-glucose positron emission tomography computed tomography (^{18}F-FDG-PET/CT) scans found that adult human BAT can be recruited after chronic cold exposure even in subjects who do not possess appreciable amounts of BAT depots before cold exposure; this recruitment of BAT is accompanied by an increase in energy expenditure and improved postprandial insulin sensitivity (Lee et al., 2014a; van der Lans et al., 2013; Yoneshiro et al., 2013). Furthermore, molecular analyses indicate that adult human BAT contains beige-like adipocytes (Cypess et al., 2013; Lee et al., 2014b; Lidell et al., 2013; Sharp et al., 2012; Shinoda et al., 2015; Wu et al., 2012; Xue et al., 2015). For instance, RNA-sequencing analyses of clonal adult human brown adipocytes indicate that their gene signatures resemble murine beige adipocytes (Shinoda et al., 2015). These results further emphasize the potential importance of beige adipocytes in human obesity and metabolic diseases.

Stimulation of β-adrenoceptor (β-AR) is a major physiological stimulus of adipocyte lipolysis in response to cold exposure. Catecholamines released from the sympathetic nerve terminals binds to β-ARs and increases intracellular cAMP levels. The increase in cAMP levels activates protein kinase A (PKA), followed by phosphorylation of hormone-sensitive lipase (HSL) and perilipin (PLIN), which stimulates lipolysis in white, brown, and beige adipocytes (Collins, 2011; Duncan et al., 2007). Previous studies have shown that PKA phosphorylation followed by p38MAPK activation induces the program, such as *Ucp1* via p38MAPK-mediated phosphorylation of ATF2 and PGC-1α (reviewed in Collins, 2011). However, molecular mechanisms, for which the β-AR signaling pathway preferentially promotes thermogenesis in brown and beige adipocytes, remain poorly understood.

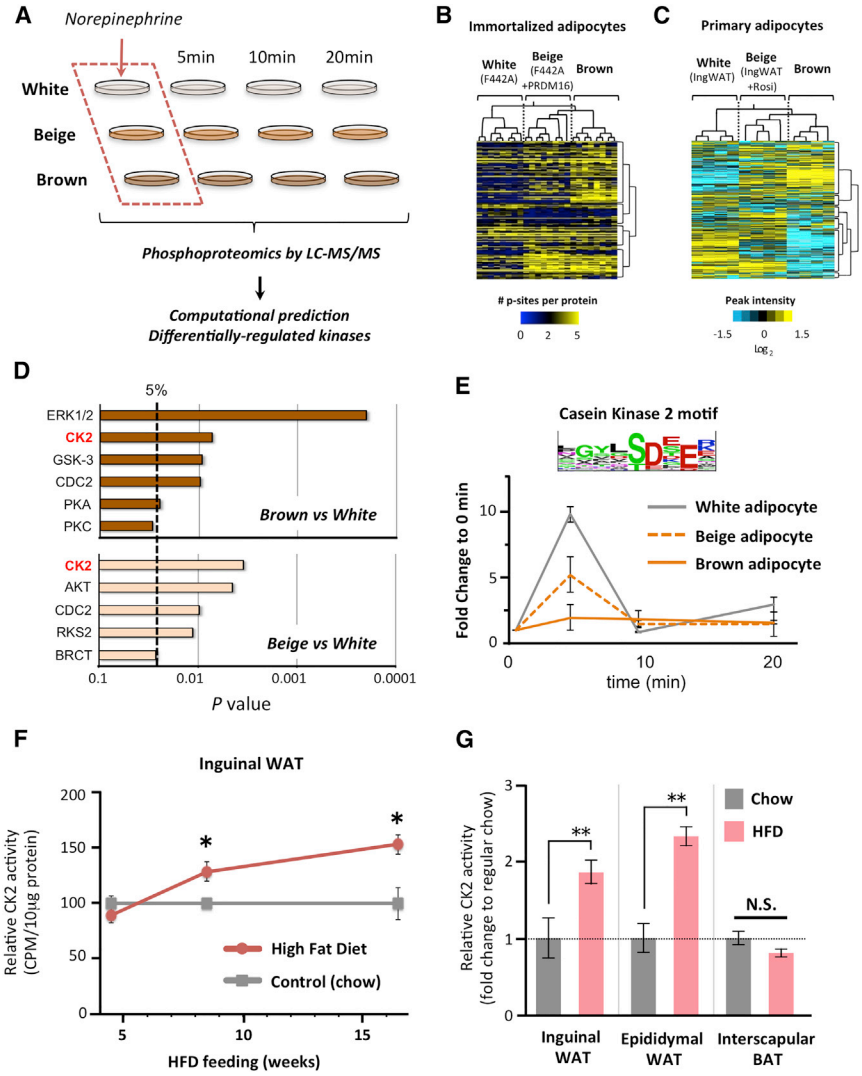

Figure 1. Identification of CK2 as a White Adipocyte-Selective Kinase Activated in Response to Norepinephrine and to a High-Fat Diet

(A) Schematic of phosphoproteomic analysis in brown, beige, and white adipocytes.

(B) Hierarchical clustering and heatmap of phosphoproteome in brown adipocytes, white adipocytes (F442A), and beige adipocytes (F442A expressing PRDM16). Each column represents sample, and each row represents phosphorylated protein. The color scale shows the numbers of phosphorylation sites per phosphoprotein in blue (low) to yellow (high) color scheme.

(C) Hierarchical clustering and heatmap of phosphoproteome in primary brown adipocytes, inguinal white adipocytes, and beige adipocytes (inguinal adipocytes treated with rosiglitazone). The color scale shows the peak intensity of phosphopeptides in $\log_2$ scale. The values are average of three measurements per sample.

(D) Phosphopeptide motif analysis of brown, beige, and white adipocytes. Brown bars represent p values by repeated-measures ANOVA to show the difference in phosphoproteome containing the indicated kinase motif between brown and white adipocytes. Beige bars represent the difference between beige and white adipocytes.

(E) Temporal dynamics of CK2 activity in brown, beige, and white adipocytes in response to norepinephrine treatment. Inset shows the conserved CK2-motif peptide sequences found in the phosphoproteome. n = 4.

(F) CK2 activity in the inguinal WAT of mice under a regular chow diet or a high-fat diet. n = 10.

(G) CK2 activity in the inguinal WAT, epididymal → WAT, and interscapular BAT of mice under a regular chow diet and a high-fat diet for 16 weeks. *p < 0.05, and **p < 0.01 by one-sided Student's t test.

Here, we employed phosphoproteomics to map global and temporal protein phosphorylation profiles in brown, beige, and white adipocytes in response to norepinephrine treatment. In contrast to conventional approaches using phosphorylation-specific antibodies, recent advances in proteomics technology allow for comprehensive profiling of protein phosphorylation from limited amounts of materials and for identifying novel functions of kinases even in seemingly well-studied signaling pathways (Blagoev et al., 2004; Krüger et al., 2008; Olsen et al., 2006). We unexpectedly found that Casein Kinase 2 (CK2), an evolutionarily-conserved serine/threonine kinase, is activated by norephinephrine stimulation preferentially in white adipocytes. Notably, blockade of CK2 by genetic or pharmacological approaches promotes the cAMP-induced thermogenesis in white adipocytes. Furthermore, inhibition of CK2 promotes beige adipocyte biogenesis in vivo and protects mice from diet-induced obesity and insulin resistance. These data provide insights on the physiological role of CK2 in the regulation of brown/beige adipocyte-selective thermogenesis and also illuminate the therapeutic potential of CK2 inhibitors in combating obesity and obesity-related diseases.

RESULTS

Phosphoproteomic Profiling of Brown, Beige, and White Adipocytes

To identify the downstream signaling pathways of norepinephrine that are unique to brown, beige, and white adipocytes, we devised a strategy as illustrated in Figure 1A. In brief, norepinephrine was added into differentiated immortalized brown adipocytes, white adipocytes (F442A cells), and a model of beige adipocytes in which PRDM16 is ectopically expressed in F442A adipocytes. The beige adipocytes express high levels of *Ucp1* and *Pgc1a* expression in response to cAMP stimuli, and low levels of WAT-selective genes (Kajimura et al., 2008). Additionally, primary stromal vascular fractions (SVFs) from the interscapular BAT and inguinal WAT were differentiated under a proadipogenic condition. Beige adipocyte differentiation was induced using rosiglitazone as previously reported (Ohno et al.,

2012). The differentiated adipocytes were harvested before the treatment (time point 0) and at 5, 10, and 20 min after norepinephrine treatment. Phosphorylated proteins from each cell type were analyzed by liquid chromatography coupled with tandem mass spectrometry (LC-MS/MS). Subsequently, the identified phosphopeptides were computationally analyzed to predict the kinases responsible for the adipose-selective phosphorylation profiles.

To compare phosphorylation profiles, hierarchical clustering was applied based on the numbers of phosphorylation sites per phosphoprotein. The clustering analysis in Figure 1B found that expression of PRDM16 in F442A white adipocytes dramatically changed the phosphorylation profile of white adipocytes to a profile resembling that of brown adipocytes. The complete phosphoproteome data sets are found in Table S1 available online. In primary adipocytes, the phosphoproteome profile of beige adipocytes resembles that of classical brown adipocytes even when we applied the hierarchical clustering based on the phosphopeptide peak intensity (Figure 1C). These analyses capture the downstream signaling events of norepinephrine that are unique to thermogenic adipocytes (i.e., brown and beige adipocytes).

CK2 Pathway Is Preferentially Activated in White Adipocytes in Response to Norepinephrine and to an Obesogenic Diet

To predict kinases responsible for the adipose-selective phosphorylation profile, we first searched for conserved phosphopeptide motifs from the above phosphoproteome. Next, the PhosphoMotif finder database (Amanchy et al., 2007) was applied to predict kinase families that were known to phosphorylate such phosphopeptide motifs. Next, relative activities of the predicted kinases were quantified by counting the consensus phosphopeptide motifs at each time point. These analyses identified five kinases, including extracellular signal-related kinase (ERK1/2), CK2, glycogen synthase kinase-3 (GSK-3), cyclin division cycle 2 (CDC2), and PKA that were significantly different between brown versus white adipocytes (Figure 1D). Of note, previous studies report that norepinephrine activates Erk1/2 (Lindquist and Rehnmark, 1998; Shimizu et al., 1997; Valladares et al., 2000) and PKA (Cao et al., 2001; Fredriksson et al., 2001) signaling in brown adipocytes. Similarly, four kinases, including CK2, AKT, CDC2, and ribosomal S6 kinase alpha3 (RKS2), displayed significantly different profiles in beige versus white adipocytes. Among them, CK2 exhibited differential activity between thermogenic adipocytes versus white adipocytes. As shown in Figure 1E, levels of the CK2 motif-containing phosphopeptides were dramatically increased in white adipocytes, but not in brown adipocytes, in response to norepinephrine treatment. This increase was seen in a much lesser extent in beige adipocytes than white adipocytes. Temporal phosphorylation patterns of PKA, GSK3 and CDC2 are shown in Figure S1A. A similar trend of the CK2 phosphopeptide profile was observed in primary adipocytes (Figure S1B).

To examine if CK2 is regulated under obesity, CK2 activity was measured in the adipose tissues of mice under a high-fat diet or a regular diet. While no difference was observed at 4 weeks of high-fat diet, CK2 activity was significantly increased in the inguinal and epididymal WAT at 8 and 16 weeks of high-fat diet as compared to those under a regular diet (Figures 1F and S2A). Importantly, such an increase was selective to the WAT depots, as CK2 activity was not changed in the interscapular BAT (Figure 1G). The obesity-associated increase in CK2 activity occurs primarily in SVFs (Figure S2B), although no significant change was observed in the SFVs from WAT after cold exposure (Figure S2C). Higher CK2 activity under obesity was due, in part, to an increase in mRNA expression of *Ck2α1*, *Ck2α2*, and *Ck2β* (Figure S2D), as CK2 activity is highly regulated at the level of *Ck2α* gene expression (Allende and Allende, 1995; Li et al., 1999). These results indicate that the CK2 pathway is activated preferentially in WAT in response to an obesogenic diet and norepinephrine.

Depletion of CK2 Activates the cAMP-Induced Thermogenic Program in White Adipocytes

CK2 is a serine/threonine kinase that is composed of catalytic subunits (α1 and α2) and two regulatory β subunits. To examine the roles of CK2 in the regulation of adipocyte thermogenesis, each CK2 subunit was depleted by RNAi in inguinal WAT-derived immortalized white adipocytes. The mRNA levels of α1, α2, and β subunits were significantly decreased by 76%, 74%, and 77%, respectively (Figure 2A). Notably, depletion of the major catalytic component of CK2 (*Ck2α1*) significantly increased *Ucp1* and *Pgc1a* mRNA expression when differentiated white adipocytes were stimulated with forskolin (Figure 2B). Depletion of *Ck2α2* also increased *Ucp1* expression, albeit moderately. Knockdown of *Ck2β* subunit significantly impaired adipogenesis, as assessed by *Fabp4* expression. Of note, *Ucp1* expression was robustly induced by forskolin treatment in the *Ck2α1*-depleted white adipocytes in a dose-dependent fashion (Figure 2C). *Ck2α1* knockdown also increased expression of the brown/beige fat-selective genes, such as *Cidea*, *Cited1*, *Cox8b*, and *Elov3*, without affecting the expression of *Fabp4* (Figure 2D). Higher UCP1 protein expression was observed in the *Ck2α1*-depleted white adipocytes under cAMP stimulation (Figure 2E), which lead to a significant increase in total and oligomycin-insensitive cellular respiration (Figure 2F). These results suggest that CK2 acts as a negative regulator of cAMP-induced thermogenesis in white adipocytes.

Pharmacological Inhibition of CK2 Promotes Beige Adipocyte Biogenesis In Vivo

To ask if blockade of CK2 promotes the thermogenic program in WAT in vivo, we administrated a potent and selective CK2 inhibitor, CX-4945, in mice under ambient temperature. CX-4945 is a newly developed orally available ATP-competitive inhibitor for CK2α1 and CK2α2 catalytic subunits, which has a strong antitumor efficacy in breast cancers, pancreatic cancers, prostate cancers, glioblastoma, and chronic lymphocytic leukemia (Bliesath et al., 2012; Martins et al., 2014; Siddiqui-Jain et al., 2010; Son et al., 2013; Zheng et al., 2013). As shown in Figure 3A, CK2 activity in the inguinal WAT was significantly reduced by 63% after a 5 day treatment at 50 mg kg^{-1}. Although CX-4945 is reported to inhibit fetal liver kinase 2 (*Flt3*) at a higher dose (Siddiqui-Jain et al., 2010), *Flt3* expression was not detected in adipose tissues (Figure S3A). Hence, CX-4945 is primarily through inhibition of CK2 in adipose tissues. As shown in Figure 3B, pharmacological inhibition of CK2 by CX-4945

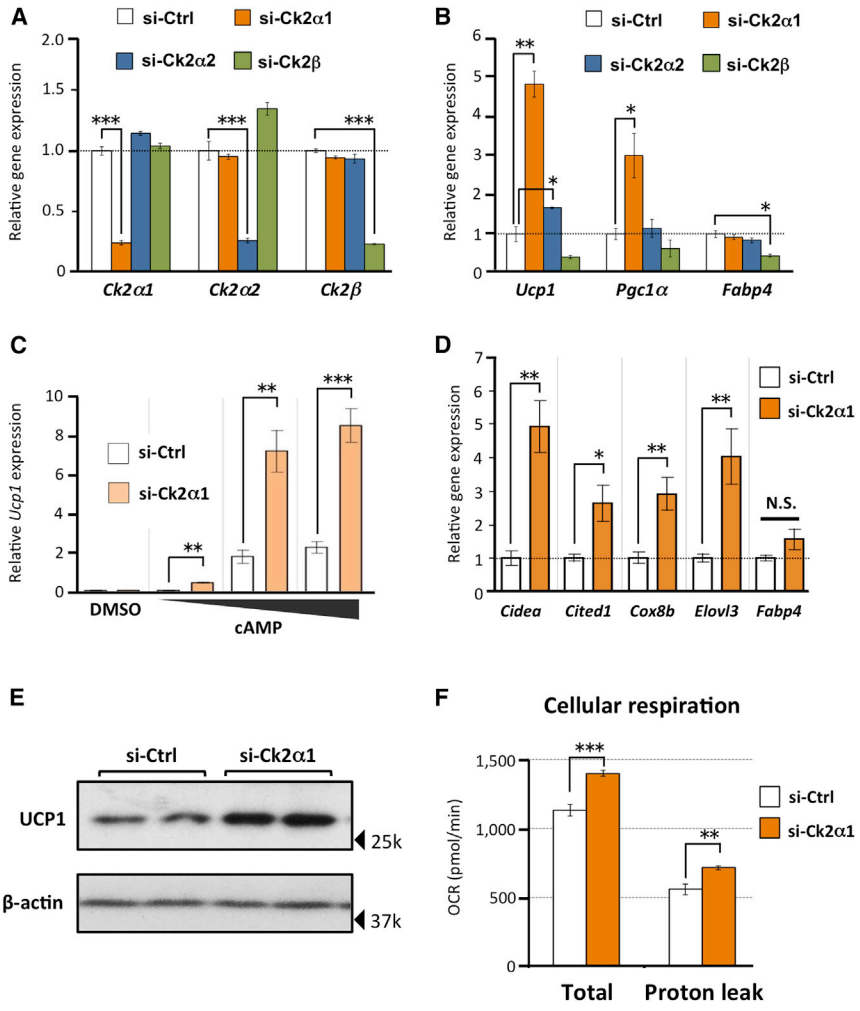

Figure 2. Depletion of CK2 Activates the cAMP-Induced Thermogenic Program in White Adipocytes

(A) Expression of *Ck2α1*, *Ck2α2*, and *Ck2β* in inguinal adipocytes transfected with siRNAs targeting the indicated subunits or non-targeting control (Ctrl). n = 3.

(B) Expression of thermogenic and adipogenic genes in inguinal white adipocytes depleted with each CK2 subunit. The cells were treated with forskolin at 10 μM for 4 hr to activate thermogenesis. n = 3.

(C) *Ucp1* expression in inguinal white adipocytes transfected with *Ck2α1*-targeting or control siRNAs. Differentiated cells were treated with forskolin at 1, 10, and 50 μM for 4 hr. n = 3.

(D) Expression of brown/beige fat-selective genes in inguinal white adipocytes transfected with *Ck2α1*-targeting or control siRNAs. n = 3.

(E) Western blotting for UCP1 in inguinal white adipocytes transfected with *Ck2α1*-targeting or control siRNAs. Differentiated cells were treated with forskolin at 10 μM for 8 hr. β-actin was used as a loading control.

(F) Cellular oxygen consumption rate (OCR) in inguinal white adipocytes transfected with *Ck2α1*-targeting or control siRNAs. Differentiated cells were treated with forskolin at 10 μM. n = 8. *p < 0.05, **p < 0.01, ***p < 0.001 by one-sided Student's t test.

significantly increased mRNA expression of *Ucp1*, *Dio2*, *Pgc1α*, *Elovl3*, *Cited1*, *Otop1*, and *Cidea* in the inguinal WAT. The increase in *Ucp1* mRNA by CK2 inhibition was accompanied by an increase in UCP1 protein expression in the inguinal WAT (Figure 3C). We also observed a moderate increase in UCP1 mRNA and protein expression in the interscapular BAT (Figures 3C and S3B). Importantly, the inguinal WAT of mice treated with CX-4945 contained abundant clusters of UCP1-positive beige adipocytes with multilocular lipid droplets as compared to that of vehicle-treated mice (Figures 3D and 3E).

To ask if the CK2 inhibitor acts in a cell-autonomous fashion, inguinal white preadipocytes were differentiated in the presence of two distinct classes of CK2 inhibitor, CX-4945 and CK2-VIII. Consistent with the knockdown studies, pharmacological inhibition of CK2 by CX-4945 significantly increased *Ucp1* expression in the presence of forskolin (Figure 3F). CK2-VIII is a highly selective CK2 inhibitor with a distinct chemical structure from CX-4945, and potently inhibits CK2 activity with IC_{50} 1.6–2.6 μM in cultured cells (Hou et al., 2012). We found that *Ucp1* mRNA expression was significantly higher in the inguinal white adipocytes treated with CK2-VIII at 1 μM (Figure 3F). Of note, the increase in *Ucp1* expression by CK2-VIII was completely blunted when endogenous *Ck2a1* was depleted in white adipocytes (Figure S3C), indicating that the cell-autonomous action of CK2-VIII is largely mediated by CK2. In addition to *Ucp1*, CX-4945 and CK2-VIII increased several brown/beige fat-selective genes, including *Pgc1α*, *Cidea*, *Elov3*, and *Cited1*, without affecting *Fabp4* expression (Figures 3G and 3H). CK2-VIII treatment also significantly increased total and oligomycin-insensitive cellular respiration when cells were stimulated with cAMP (Figure S3D). There appears to be no major change in PKA signaling by CK2 inhibition, because CKII-VIII did not change the phosphopeptide levels of major PKA targets in adipocytes, including HSL and PLIN1 (Figures S3E and S3F). Collectively, these data indicate that pharmacological inhibition of CK2 in white adipocytes activates the cAMP-induced thermogenic program in a cell-autonomous fashion.

CK2 Blockade Promotes Thermogenesis in White Adipocytes through Reduced CK2-Mediated Phosphorylation of Class I HDACs

To understand the mechanisms by which CK2 inhibition promotes cAMP-induced thermogenesis in white adipocytes, we employed phosphoproteomics to identify downstream mediators of CK2 in inguinal white adipocytes that were treated with CK2-VIII and forskolin. Hierarchical clustering analysis, as determined by the abundance of phosphorylation sites, identified a distinct cluster in which phosphorylation was significantly decreased by CK2-VIII (i.e., CK2-dependent phosphoproteins) (Figure 4A, left). The cluster was further divided into two groups

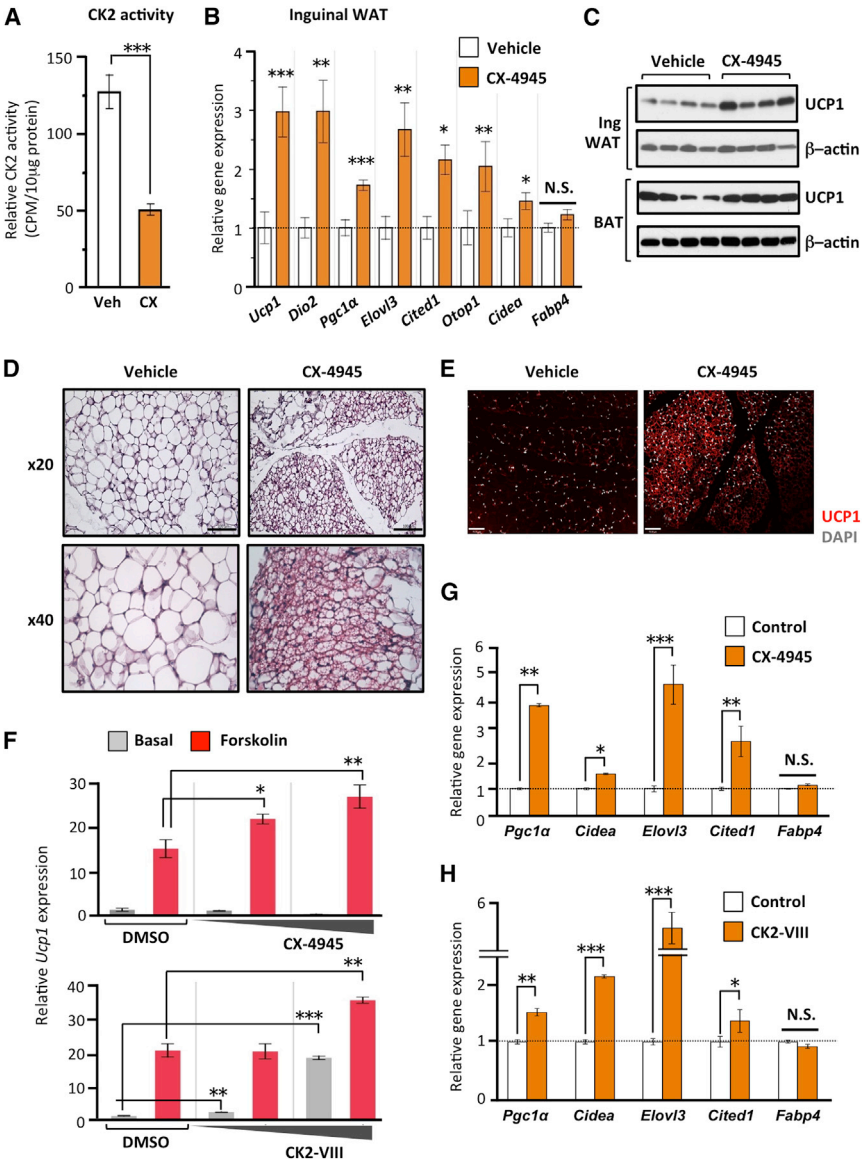

Figure 3. Pharmacological Inhibition of CK2 Promotes Beige Adipocyte Biogenesis In Vivo

(A) CK2 activity in the inguinal WAT of mice treated with vehicle or CX-4945 at 50 mg kg^{-1} twice daily for 5 days. n = 5.

(B) Expression of brown/beige fat-selective genes in the inguinal WAT of mice treated with vehicle or CX-4945 for 5 days. n = 5.

(C) Western blotting for UCP1 in the interscapular BAT and inguinal WAT in (B). β-actin was used as a loading control.

(D) H&E staining of the inguinal WAT of mice treated with vehicle or CX-4945. Bottom shows high-magnification images. Scale bar, 100 μm.

(E) UCP1 immunostaining (red) of the inguinal WAT in (D). DAPI (white) was used to stain nuclei. Scale bar, 70 μm.

(F) Dose-dependent increase in *Ucp1 mRNA* expression in inguinal white adipocytes treated with CX-4945 at 20 nM and 100 nM (top) and CK2-VIII at 0.1 and 1 μM (bottom). Differentiated adipocytes were treated with 10 μM forskolin for 4 hr. n = 3.

(G) Expression of brown/beige adipocyte-selective genes in cultured inguinal white adipocytes treated with CX-4945 at 100 nM. n = 3.

(H) Expression of brown/beige adipocyte-selective genes in cultured inguinal white adipocytes treated with CK2-VIII at 1 μM. n = 3. *p < 0.05, **p < 0.01, ***p < 0.001 by one-sided Student's t test.

in which phosphorylation was increased or decreased/unchanged by cAMP. Z-score intensities of the cAMP-stimulated cell were, on average, higher than control cells by 1.61, whereas the difference in the second cluster was −1.04. When the CK2-dependent phosphoproteins were overlapped with the phosphoproteome from brown, beige, and white adipocytes (shown in Figure 1B), we found that a large part of the CK2-dependent phosphoproteins was substantially lower in beige adipocytes (59.7%) as well as in brown adipocytes (61.1%), as compared to white adipocytes (Figure 4A, right panel). These results further support the notion that CK2 is a major regulator of the white adipocyte-selective phosphoprotein profile.

To identify direct CK2 substrates in white adipocytes, we performed in vitro kinase assays using white adipocyte-derived protein extracts, as illustrated in Figure 4B. The phosphoproteome analysis identified approximately 800 phosphorylated proteins in which 219 proteins were enriched in at least one Gene Ontology (GO) (Table S2). The GO analysis found that 46% of them were linked to cell cycle control, in addition to apoptosis (22%), ubiquitination proteolysis (19%), PI3K/AKT signaling (9%), and DNA methylation/transcription (4%) (Figure 4C). Importantly, a large part (52.8%, 308/583 proteins) of the CK2-dependent phosphoproteins found in cultured white adipocytes were direct targets of CK2 (Figure 4D). Among the putative CK2 substrates, we found that phosphorylation of class I HDACs (HDAC1 and HDAC2) was reduced by the CK2 inhibitor (Figure 4E). Specifically, three phosphorylated sites in HDAC1 at serines 393, 421, and 423 and two sites in HDAC2 at serines 422 and 424 exhibited significant changes in a CK2-dependent fashion (Figure 4F). These serine sites are evolutionarily conserved among mammalian species (Figure 4G). CK2 is known to phosphorylate HDAC2 at serines 394, 422, and 424 (Eom et al., 2011; Tsai and Seto, 2002), and mutations of HDAC1 at serines 421 and serine 423 to alanine reduce enzymatic activity and complex formation (Pflum et al., 2001).

Since inhibition of class I HDACs is known to increase PGC1a expression and oxidative metabolism (Galmozzi et al., 2013), we hypothesized that class I HDACs mediate the CK2-linked adipocyte thermogenesis. To test this, inguinal white adipocytes were incubated with CK2-VIII in the presence or absence of a class I HDAC-selective inhibitor, Mocetinostat. Similarly, the cells were cotreated with Tubastatin, a selective inhibitor of HDAC6

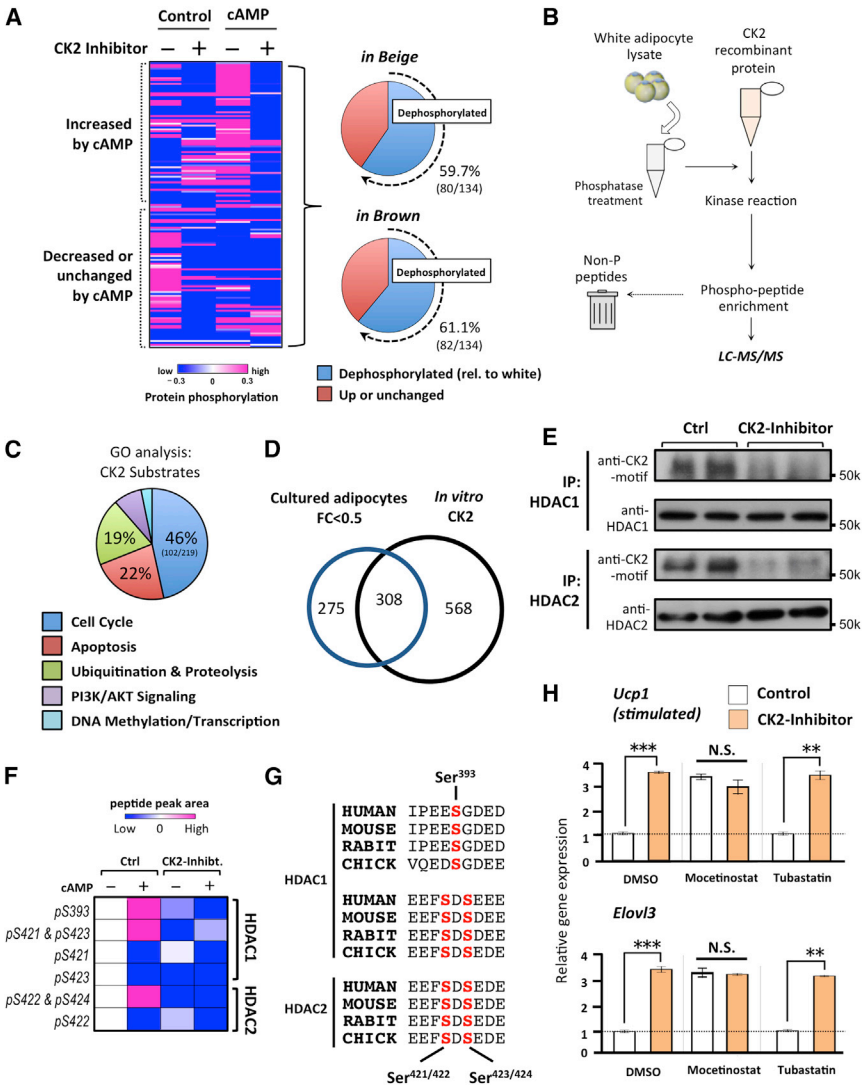

Figure 4. CK2 Blockade Activates Thermogenesis in White Adipocytes through Reduced CK2-Mediated Phosphorylation of Class I HDACs

(A) CK2-dependent phosphoproteome in white adipocytes. The color scale shows *z*-scored peak area of phosphopeptides in blue (low) to white to red (high) scheme. Pie charts show overlaps in the phosphoproteome between CK2 inhibitor-treated white adipocytes and beige adipocytes (up) or between CK2 inhibitor-treated white adipocytes and classical brown adipocytes (bottom).

(B) Schematic of in vitro CK2 substrate profiling by LC-MS/MS.

(C) GO analysis of phosphoproteins identified by in vitro CK2 substrate profiling in white adipocytes. The area of each pie slice represents the number of proteins that belong to the enriched GO terms ($p < 0.01$).

(D) Venn diagram of the overlapped phosphoproteins identified by in vivo assay in (A) and in vitro CK2 substrate profiling in (B).

(E) Phosphorylation status of class I HDACs in white adipocytes treated with CK2-VIII for 4 days. CK2-mediated phosphorylation of HDAC1 or HDAC2 was assessed by immunoprecipitation of respective antibodies followed by western blotting for phosphorylated CK2-substrate motifs. Total HDAC1 and HDAC2 proteins (input) were shown in the bottom panels. The HDAC-immunoprecipitates and input were derived from the identical samples and loaded into the separate gels.

(F) Quantification of phosphorylation in HDAC1 and HDAC2 at indicated sites in inguinal white adipocytes incubated with CK2-VIII in the presence or absence of forskolin at 10 μM.

(G) Conservation of phosphorylation sites on HDAC1 and HDAC2 in human, mouse, rabbit, and chicken.

(H) *Ucp1* and *Elovl3* mRNA expression in inguinal white adipocytes incubated with CK2-VIII in the presence or absence of Mocetinostat at 150 nM and Tubastatin at 150 nM for 4 days. Differentiated adipocytes were treated with 10 μM forskolin for 4 hr. n = 3. $^{**}p < 0.01$, $^{***}p < 0.001$ by one-sided Student's t test.

that is one of the class II HDACs but not a CK2 substrate in adipocytes. As shown in Figure 4H, CK2-VIII treatment induced *Ucp1* expression when adipocytes were stimulated with forskolin. Such increase was largely blunted when cells were co-treated with Mocetinostat. In contrast, the CK2 inhibitor-induced *Ucp1* expression was not affected in cells co-treated with Tubastatin. Similarly, the CK2 inhibitor's effect on *Elovl3* expression was not seen when cotreated with Mocetinostat (Figure 4H). These results indicate that reduced phosphorylation of class I HDACs mediates a large part of the CK2 inhibitor's effects on the thermogenetic gene program in adipocytes.

Pharmacological Blockade of CK2 Stimulates UCP1-Dependent Thermogenesis and Ameliorates Diet-Induced Obesity and Insulin Resistance

Since a functional hallmark of brown/beige fat is cold-stimulated thermogenesis, we asked if pharmacological inhibition of CK2 alters whole-body energy expenditure under cold. To this end, we measured whole-body oxygen consumption rate (VO_2) in mice treated with vehicle or CX-4945 for 5 days under different environmental temperatures. While VO_2 levels were not affected by CX-4945 treatment at thermoneutrality (30°C), the CX-4945-treated mice exhibited significantly higher energy expenditure when mice were housed progressively under cold (Figure 5A). For instance, VO_2 levels of CX-4945-treated mice were higher than vehicle-treated mice by 8% and 11.8% under 10°C and 4°C, respectively. This increase in energy expenditure was independent of food consumption and behavior (Figure S4A). Importantly, the increase in VO_2 level by CX-4945 was completely blunted in *Ucp1* null mice (Figure 5B), suggesting that a large part of the increased energy expenditure by CK2 inhibition depends on UCP1-mediated thermogenesis, rather than heat loss.

To examine therapeutic potential of pharmacological CK2 inhibition on diet-induced obesity in vivo, C57BL/6J male mice were

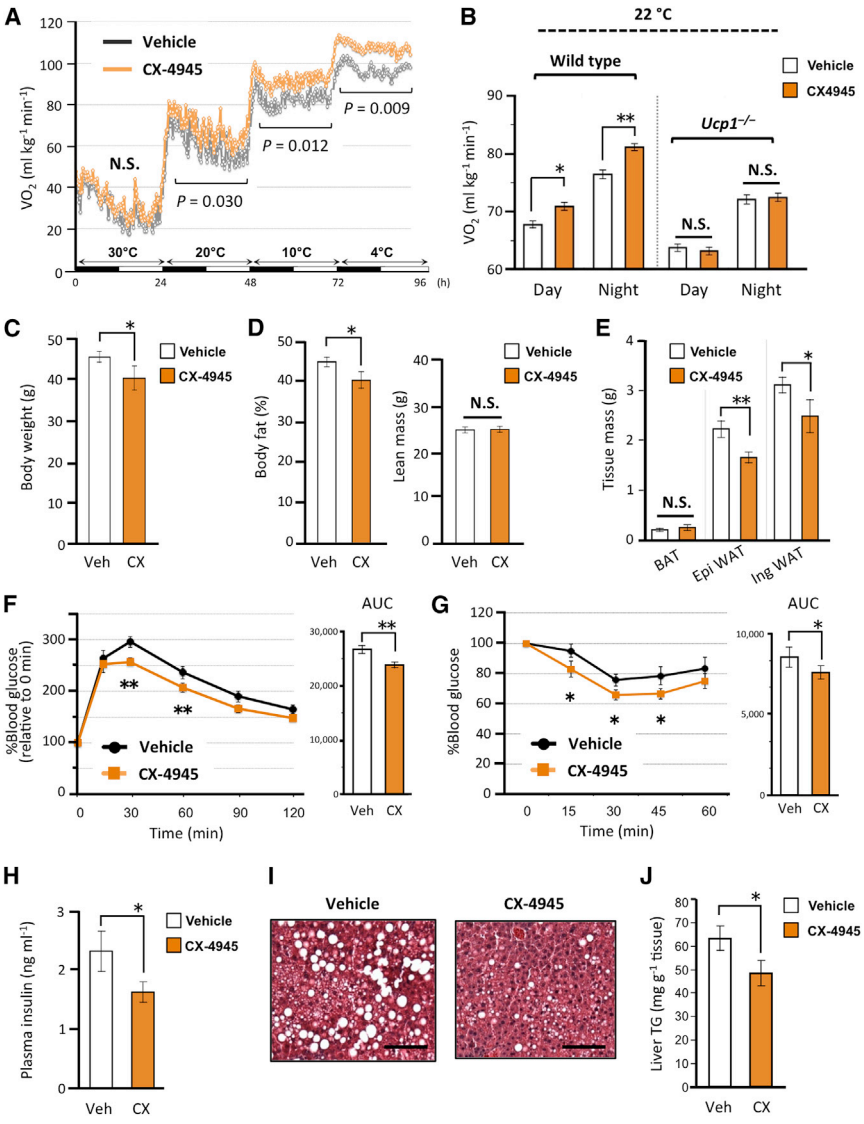

Figure 5. CK2 Blockade Stimulates UCP1-Dependent Thermogenesis and Ameliorates Diet-Induced Obesity and Insulin Resistance

(A) VO_2 of mice treated with vehicle and CX-4945 at indicated temperature. n = 5. p values were determined by repeated-measures ANOVA.

(B) VO_2 of wild-type (left) and *Ucp1* null mice (right) treated with vehicle and CX-4945 under 22°C. n = 5.

(C) Body weight of mice after treated with vehicle or CX-4945 for 40 days under a high-fat diet. n = 6.

(D) Body fat percentage (left) and lean mass (right) of mice in (C) as assessed by Echo-MRI.

(E) Weight of adipose tissues of mice in (C).

(F) Glucose tolerance test in mice in (C). AUC is shown in the right panel.

(G) Insulin tolerance test in mice in (C). AUC is shown in the right panel.

(H) Fasting plasma insulin concentration in obese mice treated with vehicle or CX-4945 for 40 days under a high-fat diet. n = 5.

(I) H & E staining of liver from mice treated with vehicle or CX-4945 for 40 days under a high-fat diet. Scale bar, 100 μm.

(J) Liver triglyceride contents in mice in (I). n = 5

*p < 0.05, **p < 0.01 by one-sided Student's t test.

fed a high-fat diet for 16 weeks and subsequently treated with vehicle or CX-4945 at 50 mg kg^{-1} over a period of 40 days. Consistent with the timing of WAT browning by CX-4945 in vivo, a significant decrease in body weight gain was observed at 10 days of CX-4945 treatment and thereafter (Figure S4B). Long-term treatment with CX-4945 was effective to prevent diet-induced body weight gain (Figure 5C). Echo-MRI analysis showed that CX-4945 treatment significantly reduced body fat mass without affecting lean body mass (Figure 5D). CX-4945 treatment significantly reduced adipose mass of the epididymal and inguinal WAT depots (Figure 5E).

We further examined if a reduced body weight gain by CK2 inhibition leads to an improvement in systemic glucose homeostasis. Glucose tolerance test (GTT) found that mice treated with CX-4945 exhibited moderately but significantly lower blood glucose levels than vehicle-treated mice (Figure 5F). Insulin tolerance test (ITT) showed that CX-4945 treated mice displayed significantly improved response to insulin (Figure 5G) and lower serum insulin levels under a fasted state (Figure 5H) than vehicle-treated mice. Since recent studies indicate a close connection between BAT thermogenesis and hepatic lipid metabolism (Bartelt et al., 2011; Cohen et al., 2014; Ohno et al., 2013), we examined the liver phenotype of mice treated with CX-4945. We found that the liver from mice treated with CX-4945 contained significantly lower amounts of lipid droplets (Figure 5I) and triglyceride (Figure 5J), as compared to vehicle-treated mice. These results indicate that pharmacological CK2 inhibition ameliorates diet-induced obesity and insulin resistance by promoting UCP1-dependent thermogenesis.

Antisense Oligonucleotide-Based Depletion of CK2 Synergistically Promotes Beige Adipocyte Biogenesis under Mild Cold Exposure

We employed antisense oligonucleotide (ASO) as an alternative approach to selectively block CK2 in vivo. When wild-type mice were treated with ASO targeting *Ck2α1* (Ck2-ASO) or control ASO at 40 mg kg^{-1} twice a week, *Ck2α1* mRNA level was significantly reduced by 70% in inguinal WAT, while expression of *Ck2α2* and *Ck2beta* was unaffected (Figure 6A). The reduction in *Ck2α1* mRNA level resulted in a decrease in the protein level of CK2α1 (Figure 6B) and reduction in CK2 activity by approximately 50% (Figure 6C). Furthermore, mice treated with the Ck2-ASO displayed a significant increase in whole-body energy expenditure when mice were treated with the beta3-AR agonist CL 316,243 under thermoneutrality (Figures 6D and S5A).

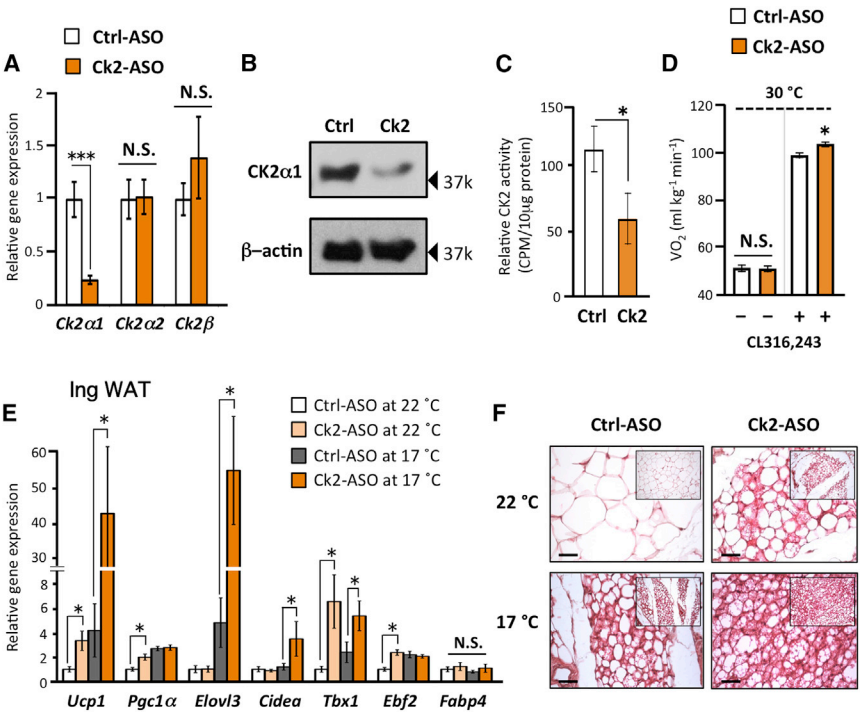

Figure 6. ASO-Based Depletion of CK2 Synergistically Promotes Beige Adipocyte Biogenesis under Mild Cold Exposure

(A) Expression of *Ck2α1*, *Ck2α2*, and *Ck2β* in the inguinal WAT of mice treated with control or Ck2-ASO. n = 9.

(B) Western blotting for CK2α1 in the inguinal WAT in (A). β-actin was used as a loading control.

(C) CK2 activity in the inguinal WAT of mice treated with control or Ck2-ASO. n = 5.

(D) VO_2 of mice injected with control or Ck2-ASOs. The mice were treated with saline or CL316,243 at 0.5 mg kg^1 under thermoneutrality. n = 5.

(E) Expression of brown/beige fat-selective marker genes in the inguinal WAT of mice treated with control or Ck2-ASO under a high-fat diet. n = 5. *p < 0.05, ***p < 0.001 by one-sided Student's t test.

(F) H&E staining of the inguinal WAT of mice in (E). Lower-magnification images are shown in insets. Scale bar, 50 μm.

Based on these results, we hypothesized that a combination of CK2 depletion and cold exposure may synergistically activate the thermogenic program. To this end, *Ck2α1* was depleted in wild-type mice under a high-fat diet either at ambient temperature (22°C) or mild cold temperature (17°C). Consistent with the previous results, *Ucp1* mRNA in inguinal WAT was elevated by 3-fold and 5-fold by Ck2-ASO treatment and mild cold exposure, respectively. Notably, Ck2-ASO treatment under mild cold exposure resulted in a robust increase in *Ucp1* expression by 43-fold (Figure 6E). Expression of other brown/beige fat-selective genes in the inguinal WAT, such as *Cidea* and *Elovl3*, followed the similar trend, while expression of *Fabp4* was not affected. We also observed a moderate increase in the expression of *Ucp1*, *Pgc1a*, *Elovl3*, and *Cox7a1* in the interscapular BAT by Ck2-ASO and mild cold exposure (Figure S5B). The modest effect in the interscapular BAT depot may be due to lower CK2 activity in BAT than in WAT. Histological analysis of the inguinal WAT depots found that Ck2-ASO and mild cold exposure synergistically promoted the recruitment of multilocular and UCP1-positive beige adipocytes (Figures 6F and S5C). These data suggest that ASO-mediated CK2 depletion promotes cold-induced thermogenesis in WAT.

ASO-Based CK2 Depletion Enhances Cold-Stimulated Energy Metabolism and Ameliorates Diet-Induced Obesity and Insulin Resistance

To examine the combinatorial effect of Ck2-ASO and mild cold exposure on whole-body energy metabolism, C57BL/6J male mice were fed with a high-fat diet and treated with control-ASO or Ck2-ASO under 22°C or 17°C. As shown in Figure 7A, Ck2-ASO treatment at 17°C led to a 23% reduction of diet-induced body weight gain as compared to control mice at 22°C, whereas CK2-ASO or mild cold exposure alone reduced body weight gain by 13% and 12%, respectively. No significant change in food intake was detected between Control- and Ck2-ASO treated group (Figure 7B). The changes in body weight was due to reduction in body fat mass, but not to changes in lean mass (Figure 7C).

Lastly, we assessed if Ck2-ASO improves systemic glucose homeostasis and hepatic lipid metabolism. While glucose tolerance was significantly improved in mice treated with Ck2-ASO, such improvement was further enhanced under mild cold exposure (Figures 7D and E). Insulin sensitivity was significantly improved in mice treated with Ck2-ASO both under 22°C and 17°C (Figure 7F). Fasting insulin levels were significantly reduced in mice treated with Ck2-ASO under 22°C, while Ck2-ASO treated mice under mild cold exposure displayed lower levels of fasting insulin than control-ASO treated mice under 22°C (Figure 7G). The liver from CK2-treated mice contained significantly lower levels of TG under 22°C and 17°C (Figure 7H). Together, these results indicate that ASO-mediated CK2 depletion leads to a profound improvement in adiposity, systemic glucose homeostasis, and hepatic lipid metabolism under a high-fat diet. This metabolic improvement by the CK2 inhibition is further enhanced by mild cold exposure.

DISCUSSION

From our unbiased phosphoproteomic analyses of brown, beige, and white adipocytes, we unexpectedly found that the CK2 signaling pathway is activated preferentially in white fat in response to cAMP stimuli and to an obesogenic diet. In the phosphoproteome, we used two independent cellular models of beige adipocytes that were induced by PRDM16 overexpression and chronic treatment with rosiglitazone. As a control for each model, we used UCP1-negative white adipocytes that were derived from the same source. This is because we are aware of the possibility that difference(s) in a given kinase activity is simply due to different source of cells, rather than functional

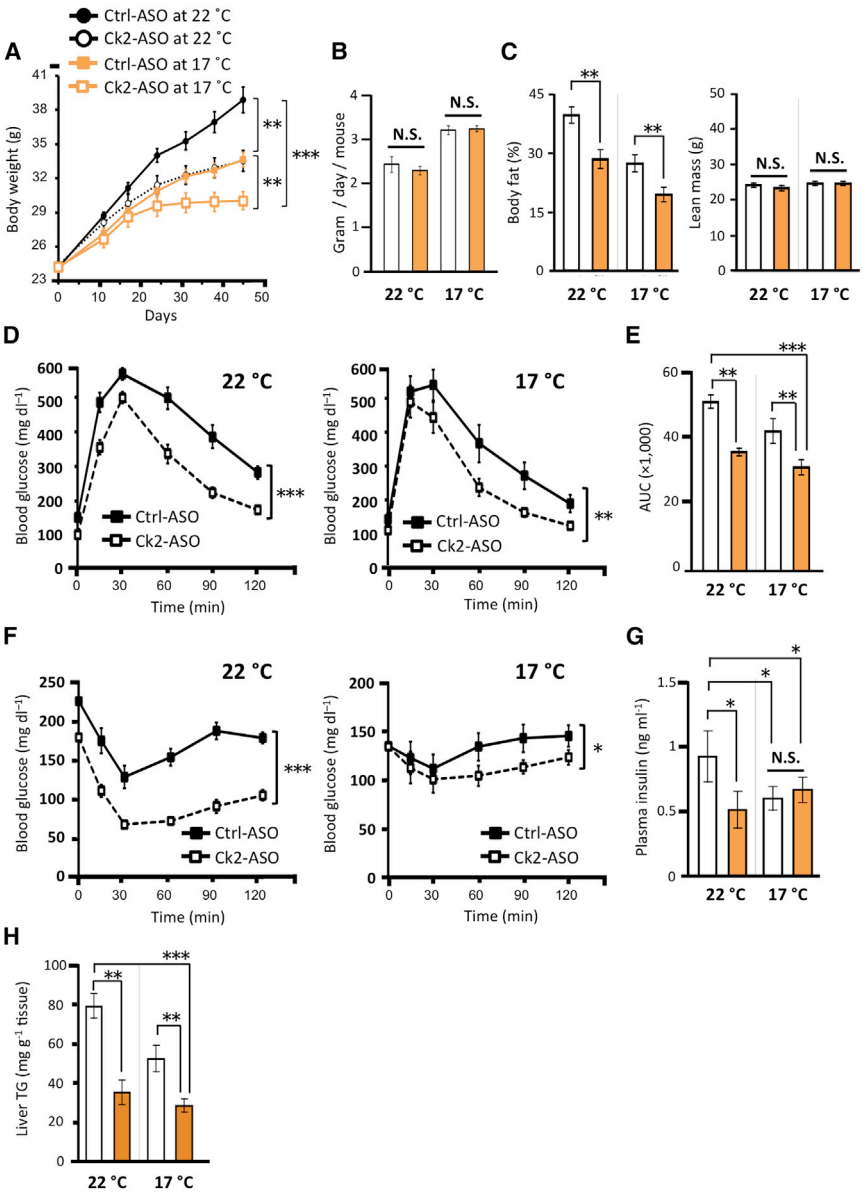

Figure 7. ASO-Based CK2 Depletion Enhances Cold-Stimulated Metabolism and Ameliorates Diet-Induced Obesity and Insulin Resistance

(A) Changes in body weight of mice treated with control or Ck2-ASOs under a high-fat diet. Mice were housed under 22°C or 17°C. n = 9.

(B) Food intake in mice treated with control or Ck2-ASOs in (A). Data are average of the first 2 weeks.

(C) Body fat percentage and lean mass in (A).

(D) GTT of mice treated with control or Ck2-ASOs in (A).

(E) AUC of GTT in (D).

(F) ITT of mice treated with control or Ck2-ASOs in (A).

(G) Fasting plasma insulin concentration of mice in (A).

(H) Liver triglyceride contents in (A). *$p < 0.05$, **$p < 0.01$, ***$p < 0.001$ versus control by one-sided Student's t test.

difference (i.e., thermogenesis). We found that CK2 activity is consistently higher in UCP1-negative white adipocytes, as compared to UCP1-postive brown/beige adipocytes in both models. Of note, genetic or pharmacological inhibition of CK2 in white fat enhances the thermogenic program in response to cAMP stimuli, while CK2 inhibition alone is not sufficient to do so. These data indicate that CK2 function as a negative regulator of cold/cAMP-induced thermogenesis in adipocytes.

The phosphoproteomics of CK2 substrates found a previously unappreciated function of CK2 in thermogenesis through phosphorylation of class I HDACs. Intriguingly, the molecular link between class I HDACs and mitochondrial biogenesis has been previously reported in skeletal muscle, cardiac muscle, and adipose tissue. As an example, cardiac-specific deletion of HDAC3 results in increased expression of mitochondrial OXPHOS genes (Montgomery et al., 2008). Furthermore, pharmacological inhibition of class I HDACs by MS-275, a clinical stage HDAC1 inhibitor, enhances oxidative metabolism in skeletal muscle and adipose tissues (Galmozzi et al., 2013). Of note, the CK2 phosphorylation deficient mutant of HDAC1 at serine 421 and serine 423 displayed reduced enzymatic activity and repressor complex formation with CoREST, MTA2, RbAp48, and Sin3A (Pflum et al., 2001). These observations indicate that inhibition of CK2-mediated phosphorylation on class I HDACs mediates a large part of the CK2 inhibitor's action on thermogenesis in white adipocytes. Our phosphoproteomics also identified novel CK2 substrates that may contribute to the CK2 inhibitor's effects, such as TLE3, PTEN, and PRDM16 that are previously reported to control brown/beige adipocyte development (Kajimura et al., 2009; Ortega-Molina et al., 2012; Seale et al., 2011, 2007; Villanueva et al., 2013). It is possible that these CK2 targets may be involved in the regulation of beige adipocyte biogenesis and thermogenesis via the CK2 pathway.

Because the β3-AR pathway plays a dominant role in stimulating BAT thermogenesis, extensive efforts have been made in the past to pharmacologically activate BAT thermogenesis using the β-AR agonists in adult humans. While some adverse effects on the cardiovascular system prevented the use of β-AR agonist in the clinic (Villarroya and Vidal-Puig, 2013), a recent study reported that oral administration of Mirabegron, a selective β3-AR agonist, significantly stimulated glucose uptake in the BAT depots in healthy adult humans who possess active BAT depots before the treatment (Cypess et al., 2015). Administration of a pan-adrenergic agonist (Ephedrine) also activates BAT metabolic activity in lean subjects (Carey et al., 2013). Given our results that CK2 inhibition enhances the UCP1-dependent thermogenesis in response to cold/β3-AR

stimuli even in diet-induced obese mice, it is conceivable that coadministration of CK2 inhibitors and β3-AR agonists, such as Mirabegron, may effectively activate BAT thermogenesis even in subjects who possess lower sensitivity to β3-AR agonists, such as obese and/or elderly populations.

EXPERIMENTAL PROCEDURES

Phosphoproteomics

Differentiated adipocytes were treated with norepinephrine at 1 μM. To determine the CK2 targets, inguinal white adipocytes were treated with CK2-VIII at 1 μM or vehicle (DMSO) for 4 days. The differentiated adipocytes were treated with forskolin at 10 μM for 20 min. Phosphoproteins, isolated from the collected adipocytes, were enriched by TiO_2-based hydroxy acid-modified metal oxide chromatography (HAMMOC) (Sugiyama et al., 2007). Phosphopeptides were desalted by StageTips (Rappsilber et al., 2007) and suspended in the loading buffer for subsequent nanoLC-MS/MS analyses.

For in vitro kinase substrate profiling, cell lysates from differentiated inguinal white adipocytes were first dephosphorylated with phosphatase at 37°C for 1 hr, followed by heat inactivation at 75°C for 30 min. Subsequently, 100 μg of the dephosphorylated proteins were reacted with recombinant CK2 (Carna Biosciences) at 37°C, and subsequently digested with Lys-C/trypsin. Phosphopeptides were analyzed by nanoLC–MS/MS system.

The phosphoproteome data were analyzed using AB Sciex MS Data Converter to create peak lists based on the recorded fragmentation spectra. Mascot v. 2.4 (Matrix Sciences) was used against SwissProt Database with the parameters previously described (Yamana et al., 2013), except for a precursor mass tolerance of 10 ppm and a fragment ion mass tolerance of 0.1 Da. The data files from the Q-Exactive system were analyzed using Mascot version 2.5.1 against SwissProt Database (version 2015_02) with a precursor mass tolerance of 5 ppm and the fragment ion mass tolerance of 0.02 Da. The number of phosphopeptides with motif was normalized to the number at basal (time point 0). Statistical evaluation was based on this normalized value using repeated-measures ANOVA. The MS proteomics data have been deposited with the dataset identifier PXD002812.

Animals

All animal experiments were performed according to procedures approved by UCSF's Institutional Animal Care and Use Committee. Male C57BL/6J mice at 4 weeks of age were fed with a regular diet (9% fat) or a high-fat diet (60% kcal% fat) for 4–18 weeks. *Ucp1*$^{-/-}$ mice in C57Bl/6J background were derived from heterozygous breeding pairs.

Metabolic Studies

CX-4945 at 50 mg kg^{-1} (Axon Medchem) was administered by oral gavage twice daily for 5 days and up to 40 days. To assess the effects of CX-4945 on whole-body energy expenditure, vehicle or CX-4945 treated mice were transferred to CLAMS chamber at 9 weeks of age. For cold challenge experiments using CX-4945, male 6-week-old C57BL6/J mice under a regular diet were acclimated to 30°C for 2 weeks and administrated with vehicle or CX-4945 for 5 days. The mice were transferred to CLAMS chamber and VO_2/O_2 were collected under 30°C, 20°C, 10°C, and 4°C. For in vivo delivery of ASO, male 8-week-old C57BL/6J mice were IP-injected with control (CCTTCCCTGAAGGTTCCTCC)- or Ck2-ASO (GTCTGTTAACGTCTGGTACA) at 40 mg kg^{-1} twice a week. To assess the metabolic effects of CX-4945 or Ck2-ASO, male obese C57BL/6J mice were fed a high-fat diet (60% fat). For GTT, the mice were injected intraperitoneally with glucose (2 g kg^{-1}) after 6 hr fasting. For ITT, the mice were injected intraperitoneally with insulin (0.75 U kg^{-1}).

CK2 Activity Assay

CK2 kinase activity assay was performed as described previously (Ruzzene et al., 2010) with minor modifications. Ten μg of protein lysates were incubated with CK2-substrate peptide (Millipore) at 30°C for 10 min in a kinase assay buffer (Millipore) in the presence of PKA inhibitors and 10 μM [γ-^{32}P]ATP (PerkinElmer). We observed a tight linear correlation ($R^2 > 0.99$) between the amounts of protein used in the assays and the CK2 activity.

RNAi Knockdown

SMARTpool ON-TARGETplus siRNA for *Ck2α1* (NM_007788), *Ck2α2* (NM_009974) and *Ck2β* (NM_009975) were obtained from GE Dharmacon. Nontargeting siRNA was used as a control. Preadipocytes were reverse transfected with siRNA using Lipofectamine RNAiMAX. Adipocyte differentiation was induced by treating confluent cells in Advanced DMEM/F-12 (Life Technologies) containing 10% FBS, 0.5 mM isobutylmethyl-xanthine, 125 μM dexamethasone, 2 μg ml-1 dexamethasone, 850 nM insulin, 1 nM T3, and 1 μM rosiglitazone. Two days after induction, cells were further incubated in a maintenance medium containing 10% FBS, 850 nM insulin, and 1 nM T3 for for 3.5 days. For cAMP treatment, cells were incubated with 10 μM forskolin for 4 or 8 hr for RNA and protein analyses, respectively.

SUPPLEMENTAL INFORMATION

Supplemental Information includes five figures and three tables and can be found with this article at http://dx.doi.org/10.1016/j.cmet.2015.09.029.

ACKNOWLEDGMENTS

We are grateful to Dr. Patrick Seale for providing the cell line, and to Dr. Yuriy Kirichok, Dr. Christophe Paillart, Kathleen Jay, Dylan Lowe, Miranda Broz, and Svetlana Keylin for their kind support. This work was supported by grants from the NIH (DK087853 and DK97441) to S.K. We also acknowledge supports from the DERC center grant (DK63720), UCSF Liver Center (P30 DK026743), the Pew Charitable Trust, and PRESTO from Japan Science and Technology Agency (also to S.K.). K.S. is supported by a fellowship from The Larry L. Hillblom Foundation. Y.H. is supported by Manpei Suzuki Diabetes Foundation. M.G. is an employee and stock holder of Isis Pharmaceuticals. H.C. is supported by a fellowship from the Japan Society for the Promotion of Science.

Received: February 27, 2015
Revised: July 21, 2015
Accepted: September 29, 2015
Published: October 29, 2015

REFERENCES

Allende, J.E., and Allende, C.C. (1995). Protein kinases. 4. Protein kinase CK2: an enzyme with multiple substrates and a puzzling regulation. FASEB J. *9*, 313–323.

Amanchy, R., Periaswamy, B., Mathivanan, S., Reddy, R., Tattikota, S.G., and Pandey, A. (2007). A curated compendium of phosphorylation motifs. Nat. Biotechnol. *25*, 285–286.

Bartelt, A., Bruns, O.T., Reimer, R., Hohenberg, H., Ittrich, H., Peldschus, K., Kaul, M.G., Tromsdorf, U.I., Weller, H., Waurisch, C., et al. (2011). Brown adipose tissue activity controls triglyceride clearance. Nat. Med. *17*, 200–205.

Blagoev, B., Ong, S.E., Kratchmarova, I., and Mann, M. (2004). Temporal analysis of phosphotyrosine-dependent signaling networks by quantitative proteomics. Nat. Biotechnol. *22*, 1139–1145.

Bliesath, J., Huser, N., Omori, M., Bunag, D., Proffitt, C., Streiner, N., Ho, C., Siddiqui-Jain, A., O'Brien, S.E., Lim, J.K., et al. (2012). Combined inhibition of EGFR and CK2 augments the attenuation of PI3K-Akt-mTOR signaling and the killing of cancer cells. Cancer Lett. *322*, 113–118.

Cao, W., Medvedev, A.V., Daniel, K.W., and Collins, S. (2001). beta-Adrenergic activation of p38 MAP kinase in adipocytes: cAMP induction of the uncoupling protein 1 (UCP1) gene requires p38 MAP kinase. J. Biol. Chem. *276*, 27077–27082.

Carey, A.L., Formosa, M.F., Van Every, B., Bertovic, D., Eikelis, N., Lambert, G.W., Kalff, V., Duffy, S.J., Cherk, M.H., and Kingwell, B.A. (2013). Ephedrine activates brown adipose tissue in lean but not obese humans. Diabetologia *56*, 147–155.

Cohen, P., Levy, J.D., Zhang, Y., Frontini, A., Kolodin, D.P., Svensson, K.J., Lo, J.C., Zeng, X., Ye, L., Khandekar, M.J., et al. (2014). Ablation of PRDM16 and beige adipose causes metabolic dysfunction and a subcutaneous to visceral fat switch. Cell *156*, 304–316.

Collins, S. (2011). β-Adrenoceptor Signaling Networks in Adipocytes for Recruiting Stored Fat and Energy Expenditure. Front. Endocrinol. (Lausanne) *2*, 102.

Cypess, A.M., White, A.P., Vernochet, C., Schulz, T.J., Xue, R., Sass, C.A., Huang, T.L., Roberts-Toler, C., Weiner, L.S., Sze, C., et al. (2013). Anatomical localization, gene expression profiling and functional characterization of adult human neck brown fat. Nat. Med. *19*, 635–639.

Cypess, A.M., Weiner, L.S., Roberts-Toler, C., Franquet Elía, E., Kessler, S.H., Kahn, P.A., English, J., Chatman, K., Trauger, S.A., Doria, A., and Kolodny, G.M. (2015). Activation of human brown adipose tissue by a β3-adrenergic receptor agonist. Cell Metab. *21*, 33–38.

Duncan, R.E., Ahmadian, M., Jaworski, K., Sarkadi-Nagy, E., and Sul, H.S. (2007). Regulation of lipolysis in adipocytes. Annu. Rev. Nutr. *27*, 79–101.

Eom, G.H., Cho, Y.K., Ko, J.H., Shin, S., Choe, N., Kim, Y., Joung, H., Kim, H.S., Nam, K.I., Kee, H.J., and Kook, H. (2011). Casein kinase-2α1 induces hypertrophic response by phosphorylation of histone deacetylase 2 S394 and its activation in the heart. Circulation *123*, 2392–2403.

Fredriksson, J.M., Thonberg, H., Ohlson, K.B., Ohba, K., Cannon, B., and Nedergaard, J. (2001). Analysis of inhibition by H89 of UCP1 gene expression and thermogenesis indicates protein kinase A mediation of beta(3)-adrenergic signalling rather than beta(3)-adrenoceptor antagonism by H89. Biochim. Biophys. Acta *1538*, 206–217.

Galmozzi, A., Mitro, N., Ferrari, A., Gers, E., Gilardi, F., Godio, C., Cermenati, G., Gualerzi, A., Donetti, E., Rotili, D., et al. (2013). Inhibition of class I histone deacetylases unveils a mitochondrial signature and enhances oxidative metabolism in skeletal muscle and adipose tissue. Diabetes *62*, 732–742.

Harms, M., and Seale, P. (2013). Brown and beige fat: development, function and therapeutic potential. Nat. Med. *19*, 1252–1263.

Hou, Z., Nakanishi, I., Kinoshita, T., Takei, Y., Yasue, M., Misu, R., Suzuki, Y., Nakamura, S., Kure, T., Ohno, H., et al. (2012). Structure-based design of novel potent protein kinase CK2 (CK2) inhibitors with phenyl-azole scaffolds. J. Med. Chem. *55*, 2899–2903.

Kajimura, S., and Saito, M. (2014). A new era in brown adipose tissue biology: molecular control of brown fat development and energy homeostasis. Annu. Rev. Physiol. *76*, 225–249.

Kajimura, S., Seale, P., Tomaru, T., Erdjument-Bromage, H., Cooper, M.P., Ruas, J.L., Chin, S., Tempst, P., Lazar, M.A., and Spiegelman, B.M. (2008). Regulation of the brown and white fat gene programs through a PRDM16/CtBP transcriptional complex. Genes Dev. *22*, 1397–1409.

Kajimura, S., Seale, P., Kubota, K., Lunsford, E., Frangioni, J.V., Gygi, S.P., and Spiegelman, B.M. (2009). Initiation of myoblast to brown fat switch by a PRDM16-C/EBP-beta transcriptional complex. Nature *460*, 1154–1158.

Krüger, M., Kratchmarova, I., Blagoev, B., Tseng, Y.H., Kahn, C.R., and Mann, M. (2008). Dissection of the insulin signaling pathway via quantitative phosphoproteomics. Proc. Natl. Acad. Sci. USA *105*, 2451–2456.

Lee, P., Smith, S., Linderman, J., Courville, A.B., Brychta, R.J., Dieckmann, W., Werner, C.D., Chen, K.Y., and Celi, F.S. (2014a). Temperature-acclimated brown adipose tissue modulates insulin sensitivity in humans. Diabetes *63*, 3686–3698.

Lee, P., Werner, C.D., Kebebew, E., and Celi, F.S. (2014b). Functional thermogenic beige adipogenesis is inducible in human neck fat. Int. J. Obes. *38*, 170–176.

Li, D., Dobrowolska, G., Aicher, L.D., Chen, M., Wright, J.H., Drueckes, P., Dunphy, E.L., Munar, E.S., and Krebs, E.G. (1999). Expression of the casein kinase 2 subunits in Chinese hamster ovary and 3T3 L1 cells provides information on the role of the enzyme in cell proliferation and the cell cycle. J. Biol. Chem. *274*, 32988–32996.

Lidell, M.E., Betz, M.J., Dahlqvist Leinhard, O., Heglind, M., Elander, L., Slawik, M., Mussack, T., Nilsson, D., Romu, T., Nuutila, P., et al. (2013). Evidence for two types of brown adipose tissue in humans. Nat. Med. *19*, 631–634.

Lindquist, J.M., and Rehnmark, S. (1998). Ambient temperature regulation of apoptosis in brown adipose tissue. Erk1/2 promotes norepinephrine-dependent cell survival. J. Biol. Chem. *273*, 30147–30156.

Martins, L.R., Lúcio, P., Melão, A., Antunes, I., Cardoso, B.A., Stansfield, R., Bertilaccio, M.T., Ghia, P., Drygin, D., Silva, M.G., and Barata, J.T. (2014). Activity of the clinical-stage CK2-specific inhibitor CX-4945 against chronic lymphocytic leukemia. Leukemia *28*, 179–182.

Montgomery, R.L., Potthoff, M.J., Haberland, M., Qi, X., Matsuzaki, S., Humphries, K.M., Richardson, J.A., Bassel-Duby, R., and Olson, E.N. (2008). Maintenance of cardiac energy metabolism by histone deacetylase 3 in mice. J. Clin. Invest. *118*, 3588–3597.

Ohno, H., Shinoda, K., Spiegelman, B.M., and Kajimura, S. (2012). PPARγ agonists induce a white-to-brown fat conversion through stabilization of PRDM16 protein. Cell Metab. *15*, 395–404.

Ohno, H., Shinoda, K., Ohyama, K., Sharp, L.Z., and Kajimura, S. (2013). EHMT1 controls brown adipose cell fate and thermogenesis through the PRDM16 complex. Nature *504*, 163–167.

Olsen, J.V., Blagoev, B., Gnad, F., Macek, B., Kumar, C., Mortensen, P., and Mann, M. (2006). Global, in vivo, and site-specific phosphorylation dynamics in signaling networks. Cell *127*, 635–648.

Ortega-Molina, A., Efeyan, A., Lopez-Guadamillas, E., Muñoz-Martin, M., Gómez-López, G., Cañamero, M., Mulero, F., Pastor, J., Martinez, S., Romanos, E., et al. (2012). Pten positively regulates brown adipose function, energy expenditure, and longevity. Cell Metab. *15*, 382–394.

Pflum, M.K., Tong, J.K., Lane, W.S., and Schreiber, S.L. (2001). Histone deacetylase 1 phosphorylation promotes enzymatic activity and complex formation. J. Biol. Chem. *276*, 47733–47741.

Rappsilber, J., Mann, M., and Ishihama, Y. (2007). Protocol for micro-purification, enrichment, pre-fractionation and storage of peptides for proteomics using StageTips. Nat. Protoc. *2*, 1896–1906.

Ruzzene, M., Di Maira, G., Tosoni, K., and Pinna, L.A. (2010). Assessment of CK2 constitutive activity in cancer cells. Methods Enzymol. *484*, 495–514.

Seale, P., Kajimura, S., Yang, W., Chin, S., Rohas, L.M., Uldry, M., Tavernier, G., Langin, D., and Spiegelman, B.M. (2007). Transcriptional control of brown fat determination by PRDM16. Cell Metab. *6*, 38–54.

Seale, P., Conroe, H.M., Estall, J., Kajimura, S., Frontini, A., Ishibashi, J., Cohen, P., Cinti, S., and Spiegelman, B.M. (2011). Prdm16 determines the thermogenic program of subcutaneous white adipose tissue in mice. J. Clin. Invest. *121*, 96–105.

Sharp, L.Z., Shinoda, K., Ohno, H., Scheel, D.W., Tomoda, E., Ruiz, L., Hu, H., Wang, L., Pavlova, Z., Gilsanz, V., and Kajimura, S. (2012). Human BAT possesses molecular signatures that resemble beige/brite cells. PLoS ONE *7*, e49452.

Shimizu, Y., Tanishita, T., Minokoshi, Y., and Shimazu, T. (1997). Activation of mitogen-activated protein kinase by norepinephrine in brown adipocytes from rats. Endocrinology *138*, 248–253.

Shinoda, K., Luijten, I.H., Hasegawa, Y., Hong, H., Sonne, S.B., Kim, M., Xue, R., Chondronikola, M., Cypess, A.M., Tseng, Y.H., et al. (2015). Genetic and functional characterization of clonally derived adult human brown adipocytes. Nat. Med. *21*, 389–394.

Siddiqui-Jain, A., Drygin, D., Streiner, N., Chua, P., Pierre, F., O'Brien, S.E., Bliesath, J., Omori, M., Huser, N., Ho, C., et al. (2010). CX-4945, an orally bioavailable selective inhibitor of protein kinase CK2, inhibits prosurvival and angiogenic signaling and exhibits antitumor efficacy. Cancer Res. *70*, 10288–10298.

Sidossis, L., and Kajimura, S. (2015). Brown and beige fat in humans: thermogenic adipocytes that control energy and glucose homeostasis. J. Clin. Invest. *125*, 478–486.

Son, Y.H., Song, J.S., Kim, S.H., and Kim, J. (2013). Pharmacokinetic characterization of CK2 inhibitor CX-4945. Arch. Pharm. Res. *36*, 840–845.

Sugiyama, N., Masuda, T., Shinoda, K., Nakamura, A., Tomita, M., and Ishihama, Y. (2007). Phosphopeptide enrichment by aliphatic hydroxy acid-modified metal oxide chromatography for nano-LC-MS/MS in proteomics applications. Mol. Cell. Proteomics *6*, 1103–1109.

Tsai, S.C., and Seto, E. (2002). Regulation of histone deacetylase 2 by protein kinase CK2. J. Biol. Chem. *277*, 31826–31833.

Valladares, A., Porras, A., Alvarez, A.M., Roncero, C., and Benito, M. (2000). Noradrenaline induces brown adipocytes cell growth via beta-receptors by a mechanism dependent on ERKs but independent of cAMP and PKA. J. Cell. Physiol. *185*, 324–330.

van der Lans, A.A., Hoeks, J., Brans, B., Vijgen, G.H., Visser, M.G., Vosselman, M.J., Hansen, J., Jörgensen, J.A., Wu, J., Mottaghy, F.M., et al. (2013). Cold acclimation recruits human brown fat and increases nonshivering thermogenesis. J. Clin. Invest. *123*, 3395–3403.

Villanueva, C.J., Vergnes, L., Wang, J., Drew, B.G., Hong, C., Tu, Y., Hu, Y., Peng, X., Xu, F., Saez, E., et al. (2013). Adipose subtype-selective recruitment of TLE3 or Prdm16 by PPARγ specifies lipid storage versus thermogenic gene programs. Cell Metab. *17*, 423–435.

Villarroya, F., and Vidal-Puig, A. (2013). Beyond the sympathetic tone: the new brown fat activators. Cell Metab. *17*, 638–643.

Wu, J., Boström, P., Sparks, L.M., Ye, L., Choi, J.H., Giang, A.H., Khandekar, M., Virtanen, K.A., Nuutila, P., Schaart, G., et al. (2012). Beige adipocytes are a distinct type of thermogenic fat cell in mouse and human. Cell *150*, 366–376.

Xue, R., Lynes, M.D., Dreyfuss, J.M., Shamsi, F., Schulz, T.J., Zhang, H., Huang, T.L., Townsend, K.L., Li, Y., Takahashi, H., et al. (2015). Clonal analyses and gene profiling identify genetic biomarkers of the thermogenic potential of human brown and white preadipocytes. Nat. Med. *21*, 760–768.

Yamana, R., Iwasaki, M., Wakabayashi, M., Nakagawa, M., Yamanaka, S., and Ishihama, Y. (2013). Rapid and deep profiling of human induced pluripotent stem cell proteome by one-shot NanoLC-MS/MS analysis with meter-scale monolithic silica columns. J. Proteome Res. *12*, 214–221.

Yoneshiro, T., Aita, S., Matsushita, M., Kayahara, T., Kameya, T., Kawai, Y., Iwanaga, T., and Saito, M. (2013). Recruited brown adipose tissue as an antiobesity agent in humans. J. Clin. Invest. *123*, 3404–3408.

Zheng, Y., McFarland, B.C., Drygin, D., Yu, H., Bellis, S.L., Kim, H., Bredel, M., and Benveniste, E.N. (2013). Targeting protein kinase CK2 suppresses prosurvival signaling pathways and growth of glioblastoma. Clin. Cancer Res. *19*, 6484–6494.